Geochemistry, Petrogenesis and Tectonic Significance of the Proterozoic Mafic Dykes from the Bomdila Area, NE Lesser Himalaya, India

Shaik A. Rashid, Javid A. Ganai, Irfan Maqbool Bhat and Naqeebul Islam

Abstract The present study documents a new set of comprehensive whole rock geochemical data of metabasic rocks from Lesser Himalayan sequence, western Arunachal Pradesh, NE India. They occur as sills and dykes within Paleoproterozoic Bomdila and Rupa Group of rocks and are metamorphosed to amphibolite grade metamorphism. Hornblende and plagioclase are the dominating minerals with minor constituents of Fe-oxides, quartz, biotite and apatite in these rocks. They are sub-alkaline tholeiitic in nature, having composition of basalt to basaltic andesite. They are enriched in LREE (light rare earth elements) and LILE (large ion lithophile elements) with depleted HFSE (high field strength elements) characteristics. The geochemical signatures e.g., Fe-enrichment, high Ti/Zr ratio (>52) but low Th/Ta ratio (0.23–0.71) and large variation in La/Yb (5.43–10.21), Zr/Y (0.15–15.14), Ti/Y (261–1133) and Zr/Nb (0.15–16.42) ratios indicate that these rocks were probably derived from an enriched lithospheric mantle source due to varying degrees of partial melting and subsequently the melt was modified by fractional crystallization of olivine, pyroxene and plagioclase rather than crustal contamination. Originally these rocks were emplaced in a continental rift tectonic environment and witnessed amphibolite grade metamorphism during Himalayan orogeny. The geochemical characteristics of the studied metabasic rocks are consistent with the Paleoproterozoic mafic rocks reported from other parts of Lesser Himalaya like Chail and Juthogh amphibolites, Garhwal flows and dykes, Mandi-Darla-Rampur volcanics indicating a same magmatic event along the Lesser Himalaya around Paleoproterozoic.

S. A. Rashid (✉) · N. Islam
Department of Geology, Aligarh Muslim University, Aligarh, India
e-mail: rashidamu@hotmail.com; shaik.rashidamu@gmail.com

N. Islam
e-mail: nislam47@gmail.com

J. A. Ganai · I. M. Bhat
Department of Earth Sciences, University of Kashmir, Srinagar, India
e-mail: jganai.ganai9@gmail.com

I. M. Bhat
e-mail: imbhat89@gmail.com

R. K. Srivastava et al. (eds.), *Dyke Swarms of the World: A Modern Perspective*,
Springer Geology, https://doi.org/10.1007/978-981-13-1666-1_11

Keywords Mafic dykes · Proterozoic geochemistry · Petrogenesis · Bomdila NE Himalaya · India

1 Introduction

Mafic dykes constitute a common expression of crustal extension and represent a major prospect by which basaltic magma is transferred from the mantle to the upper crust, a process which has operated periodically throughout the last 3.0 Ga of the earth's history. In addition, mafic dykes provide a window into the composition and evolution of the sub-continental mantle and, hence, the tectonic evolutions of the overlying continental crust (Tarney 1992). Mafic rocks of Precambrian to Eocene age are well-preserved, mainly as volcanic flows, dykes and sills, throughout the Himalayan orogenic belt (Ahmad and Bhat 1987; Ahmad et al. 1999). Ahmad et al. (1999) suggested that the age concordance of Precambrian mafic magmatism covering the northern margin of Indian plate imply that 1800–2000 Ma was a period of major crustal evolution in a rift tectonic environment. The western Himalayan magmatism is generally restricted to the Lesser Himalaya and has been the subject of extensive geological and geochemical investigations (Bhat and Ahmad 1990; Ahmad and Tarney 1991; Sahai and Srivastava 1997; Ahmad et al. 1999; Srivastava and Sahai 2001; Ahmad 2008; Srivastava et al. 2009; Bikramaditya Singh and Singh 2013; Srivastava and Samal 2018). However, in the eastern Himalaya, studies have been confined to voluminous mafic magmatism of the Siang window (Jain and Thakur 1978; Bhat 1984; Roychowdhury 1984; Bhat and Ahmad 1990; Singh 1993; Sengupta et al. 1996; Singh 2006; Singh and Bikramaditya Singh 2012). Besides, only few occurrences of mafic magmatic rocks of different geochemical characteristics are reported from western Arunachal Himalaya. Geochemical studies on Sela group mafic intrusives from Central Crystallines of western Arunachal have depleted geochemical characteristics (Srivastava et al. 2009) similar to Vaikrita amphibolites of western Garhwal Himalaya (Ahmad et al. 1999). However, metabasic rocks associated with Lesser Himalayan Sequence of western Arunachal have enriched geochemical characteristics (Bikramaditya Singh and Singh 2013; Rashid and Islam 2016) consistent with Chial and Jutogh amphibolites of western Himalaya (Ahmad et al. 1999; Ahmad 2008) and Proterozoic Basal Aravalli volcanics (Ahmad and Tarney 1994). Recently, Srivastava and Samal (2018) studied Paleoproterozoic mafic intrusive rocks from the western Arunachal Himalaya for their geochemical characteristics and petrogenesis and suggested presence of a widespread ~1.9 Ga large mafic magmatic event in the Indian shield. Not much detailed geochemical studies of metabasic dykes and sills from the Bomdila and Rupa Groups of the Lesser Himalayan sequence have been carried out earlier. Rashid and Islam (2016) have conducted preliminary geochemical characters of these mafic rocks. The aim of this paper is to study major and trace element geochemical characteristics of metabasic rocks from the Lesser Himalayan sequence and to decipher their petrogenetic processes and possible emplacement environment.

2 Geology of the Study Area

The geology of the western Arunachal Himalaya has been discussed by previous workers (Verma and Tandon 1976; Bhushan et al. 1991; Kumar 1997). In western Arunachal Pradesh, Himalaya has been divided into three major tectonic units from south to north, as the Sub-Himalaya, Lesser Himalaya and Higher Himalaya (Thakur 1986). The Sub-Himalaya or outer Himalaya consists of a thick sequence of Siwalik sedimentary rocks, and thrusts with Brahmaputra alluvium in the south along north dipping Himalayan Frontal Thrust (HFT) and towards north is in thrust contact with Lesser Himalaya along the Main Boundary Thrust (MBT). The Lesser Himalaya is represented by low-medium grade metamorphic rocks known as Lesser Himalayan Crystallines (LHC) with a minor portion of the Lesser Himalayan Sedimentary Sequence (LHS) and Gondwana Group. The LHC overlies the Gondwana Group along the Bomdila Thrust, further north the LHC is in thrust contact with the Higher Himalayan Crystallines (HHC) along the Main Central Thrust (MCT).

The study area is situated in the Lesser Himalaya, West Kameng district of Arunachal Pradesh, NE India and is bounded by many important thrust faults on either side (Fig. 1). Although many workers have studied the area and proposed different stratigraphic names (Acharyya 1971; Acharyya et al. 1975; Verma and Tandon 1976; Kumar 1997), however, on the basis of lithostratigraphy, grade of regional metamorphism and associated igneous intrusives, the Proterozoic rocks of Arunachal Himalaya have been grouped into three major tectono-stratigraphic units by Srinivasan (2001); these include Sela Group, Rupa Group and Bomdila Group. The Sela Group which is considered to be the oldest sequence (Paleoproterozoic) among the three is best exposed around Sela Pass along Bomdila-Tawang road in western Arunachal Himalaya near Bhutan border. It consists of calc-silicates, marble, kyanite-sillimanite ± staurolite polyphase deformed schists, migmatites, high-grade ortho-augen gneisses and amphibolites etc. with younger intrusions of hornblende granite (481 ± 23 Ma, Dikshitulu et al. 1995), tourmaline granite (29 ± 7 Ma, Bhalla and Bishui 1989), pegmatites and aplites. The Rupa Group of rocks belong to Mesoproterozoic and constitutes thick sequence of low to medium grade garnetiferous-biotite-muscovite schists, phyllites, sericite quartzites, calc-silicates and tremolite - actinolite marbles. Main Central Thrust (MCT) separates the Sela Group of Higher Himalayan Crystallines from Rupa Group which in turn unconformably overlies the Bomdila Group in the Lesser Himalaya. The Bomdila Group essentially comprises low to medium grade metasedimentary rocks (mainly phyllites, garnetiferous mica schists and quartzites) intruded by Paleoproterozoic Bomdila augen gneisses and metabasic dykes. The Bomdila gneiss, which has been characterized as orthogneiss on the basis of textural properties, is a batholithic dimension body occupying ~500 km^2 area in the western Arunachal Pradesh, NE India. It is characterized by medium to coarse grained, well defined porphyritic augen gneisses wherein the quartz/albite augens, measuring 1–10 cm, are wrapped with biotite and muscovite. The augen gneisses exposed around Bomdila town have been dated as 1914 ± 23 Ma by Rb/Sr technique by Dikshitulu et al. (1995) and hence are considered to be Paleoprotero-

zoic in age. Various metabasic rocks occur within Rupa and Bomdila Group rocks have discordant field relations and reaction zones noticed at number of places. These field characteristics clearly demonstrate that these metabasics are younger (Paleo-proterozoic) than host gneisses and might have intruded into the basement rocks as well.

3 Field and Petrographic Studies

The sampling locations of metabasic dykes and sills intruded in the Rupa Group (i.e., granitoids and metasediments) and Bomdila Group rocks (i.e., metasediments) of Lesser Himalaya are shown in the Fig. 1. These mafic rocks are metamorphosed to amphibolites, commonly foliated in nature and occur as intrusives in gneisses (Fig. 2a) and metasediments (Fig. 2b, c), representing the younger magmatic phase. Besides aplitic and pegmatitic dykes that intrude all phases of the granitoid plutons, two types of mafic dykes were observed in the field. First type includes circular to ovoid shaped basic rocks, ranging in size from 20 to 1 m probably representing the older basement components. Sporadic occurrences of sulphide mineral specks are observed in almost all these mafic enclaves. The other type includes the mafic intrusive rocks which occur in the form of dykes and sills within granitoid gneisses. These mafic intrusive rocks range in thickness from few meters to 10 m. Grain size variation from margin to core is conspicuous with and without amygdales. The contact between the mafic rocks and host granitoids is sharp; however, mafic rocks

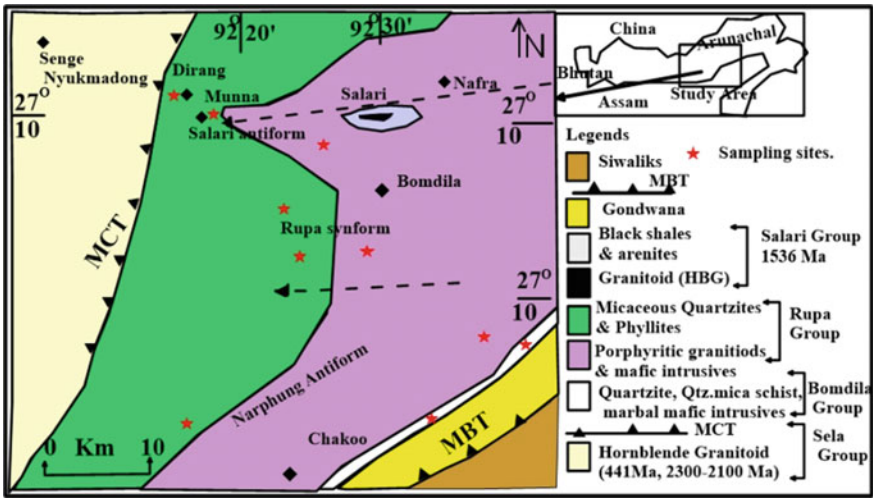

Fig. 1 Simplified geological map of the study area, western Arunachal Himalaya (after Srinivasan 2001)

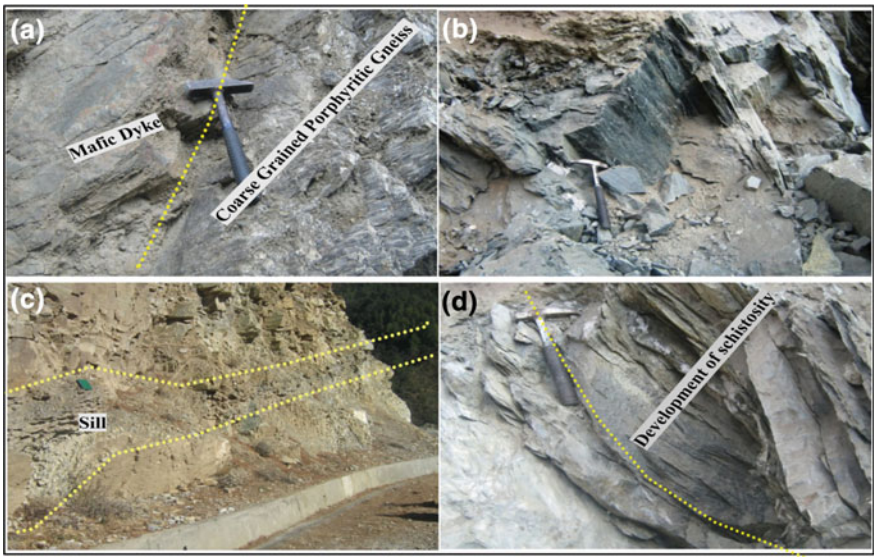

Fig. 2 Showing field relationship of Bomdila and Rupametabasic rocks within Lesser Himalaya **a** and **b** mafic dyke intruding into coarse grained porphyritic gneiss at Bomdila town, **c** mafic sill in porphyritic gneiss of Bomdila Group and **d** development of schistosity in the metabasics

have become almost schistose along the contact (Fig. 2d). At number of places, it has been observed that a marginal zone of about 1 m between granitoids and mafic rocks has been developed where considerable reaction between the two rock types has taken place. Least weathered samples of metabasic rocks from the study area were collected from the central part of the exposure, with minimum possibilities of contamination.

Photomicrographs of the studied thin sections of metabasics reveal sparsely distributed Plagioclase and hornblende phenocrysts. The chief mineral constituents are hornblende and plagioclase (oligoclase-andesine) with minor constituents of quartz and biotite. Opaques (Fe–Ti oxides), chlorite, epidote and sphene constitute minor accessory mineral phases. No garnet was observed in the studied rocks. These metabasics have pronounced schistosity which is marked by parallel orientation of hornblende and plagioclase crystals (Fig. 3a, b). At few places, recrystallization of quartz crystals with well-defined sutured margins are developed (Fig. 3b). In some thin sections, the plagioclase crystals with well-preserved twinning are encountered with biotite. Large euhedral crystals of plagioclase abut against foliated biotite; this indicates post-tectonic crystallization of plagioclase. Biotite flakes, relatively less abundant than hornblende, are aligned parallel to hornblende crystals. Subhedral epidotes are present in association with amphiboles; the epidote is secondary in nature that is formed by the breakdown of amphiboles due to late stage hydrothermal alteration. Calcite occurs as subhedral crystals and at places is associated with quartz.

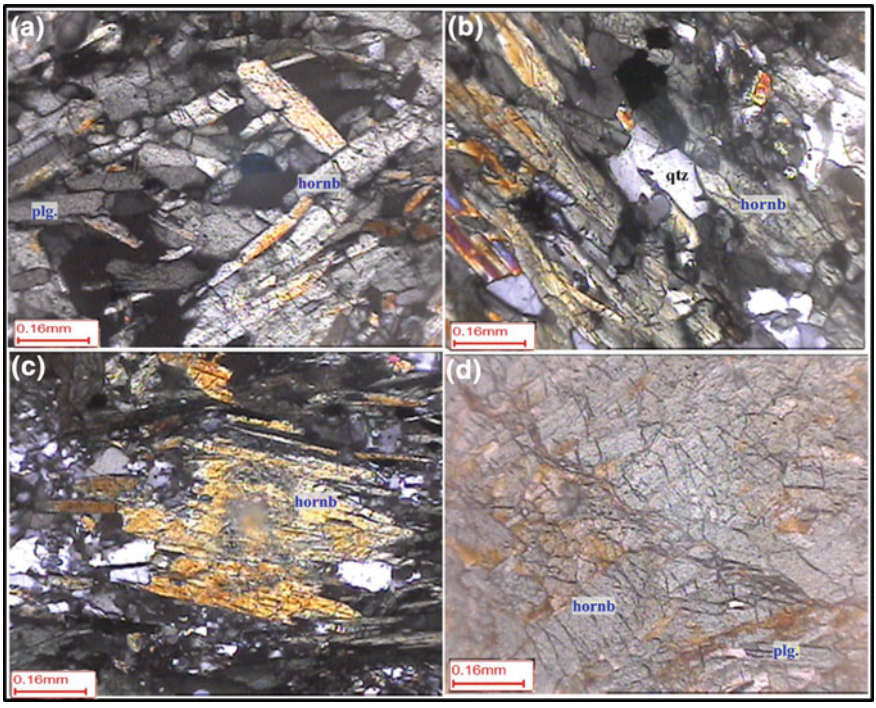

Fig. 3 Photomicrographs of Bomdilametabasic rocks from Lesser Himalaya with 5× magnification; amphibolites showing **a** and **b** the weak alignment of hornblende (hornb) and plagioclase (plg.) minerals, development of abundant hornblende and few quartz grains, **c** prismatic crystal of hornblende with two sets of cleavage, surrounded by plagioclase and opaque grains and **d** well-developed grains of hornblende and plagioclase

4 Geochemistry

4.1 Analytical Methods

After petrographic study of collected rock samples, eleven least weathered samples were selected for whole rock major and trace element analysis. All the major oxides were determined by X-ray fluorescence (XRF) spectrometry (Siemens SRS-3000 Sequential X-ray Spectrometer) at the Wadia Institute of Himalayan Geology, Dehradun, India by using pressed pellets. Accuracy and precision were obtained by repeated analysis of geostandards and evaluated by the laboratory. For XRF analyses, the accuracy at 95% confident was well within 5%while the precision was better than 3% RSD for major elements. Trace elements together with rare earth elements, were analyzed after digestion of samples with HF–HNO_3 (7:3, acid mixture) in Savillex screw-top vessels. Solutions were analyzed at National Geophysical Research Institute (NGRI), Hyderabad, by high-resolution inductively coupled mass spectrometer

(HR-ICP-MS; Nu Instruments Attom, Wrexham, United Kingdom) in jump-wiggle mode at a moderate resolution of 300, which permits all the analytes of interest to be measured accurately. Certified reference materials G-2 (USGS) and JG-2 (Japan) along with couple of procedural blanks were also prepared with the sample batch by adopting the same protocol described above to negate errors due to reagent and handling. For trace elements the procedure, precision and detection limits are the same as given by Balaram et al. (1996). The analytical results demonstrate a high degree of machine accuracy and precision better than an RSD of 3% for the majority of trace elements. The whole-rock geochemical data of studied metabasic rocks are presented in Table 1.

4.2 Post Crystallization Alteration Effects on Whole Rock Geochemistry

Prior to any interpretation of representative geochemical data, it is necessary to identify the effect of post-emplacement alteration processes on the whole-rock chemistry. Alterations like saussuritization, epidotization, silicification and chloritization occur purely as a response to progressive low-grade regional metamorphism (Condie et al. 1977). The studied rocks have undergone amphibolite grade metamorphism, which may have mobilized some of the elements. Alkali elements are the prime suspect of alteration. To elucidate the nature and the extent of migration of these alkali elements, samples were plotted in the Na_2O/K_2O versus $Na_2O + K_2O$ diagram (Fig. 4a) of Miyashiro (1975) and CaO/Al_2O_3–$MgO/10$-$SiO_2/100$ ternary diagram (Fig. 4b) of Schweitzer and Kroner (1985). It is evident from these plots that all the samples fall mainly in "not altered" field. However, slight increase in the values of Na_2O may be attributed to the albitization or spilitisation process which might have replaced Ca by Na to a varying degree. The consistent variations of majority of the major and trace elements denote that the present rocks have preserved much of their primary igneous chemistry, giving rise to acceptable intra-suite correlations for the immobile elements. Large ion lithophile elements (LILE) such as Ba, Rb, Sr etc. except Th generally show mobile nature during secondary alteration effects (Cann 1970; Pearce and Cann 1973; Condie and Sinha 1996). This effect on LILE concentrations can be revealed by Rb/Sr ratio which is very low (0.007) in least altered basaltic rocks and very high (8) in highly altered mafic rocks (Lafleche et al. 1992). The present studied metabasic samples have lower ratios of Rb/Sr (0.02–0.42) thus indicates that the secondary processes have not altered primary concentrations of LILEs. In addition, normalized REE and multielement patterns (Fig. 8) are regular and consistent suggesting that these incompatible trace element abundances and their ratios appear to reflect primary magmatic characteristics. It can be inferred from the above observations that though most of the elements in mafic rocks show their primary igneous signatures, some nonsystematic variations, however, warrant a caution against the relying too much on major element data while using for petrogenetic interpretation.

Table 1 Major oxides and trace element concentrations of metabasic rocks from the Bomdila and Rupa Group rocks of Lesser Himalaya, western Arunachal Himalaya

Major oxide (wt%)	BG-57	BG-5A	BG-58	BG-58A	BG-60	BG-61	BG-59	BG-79	DG-8(AR)	DG-11	RG-33C
SiO_2	53.52	51.01	44.82	52.92	46.64	49.09	52.54	47.91	46.3	46.46	50.17
TiO_2	1.72	1.42	1.32	2.49	2.17	2.27	2.41	3.15	3.6	2.07	2.73
Al_2O_3	12.55	12.05	11.76	12.15	12.22	11.44	13.67	11.92	12.28	12.66	13.66
$Fe_2O_3^t$	14.55	13.96	16.13	15.72	15.64	15.13	10.94	16.28	15.93	15.64	14.6
MnO	0.24	0.23	0.24	0.21	0.21	0.18	0.14	0.24	0.23	0.23	0.21
MgO	4.1	7.23	7.91	7.66	6.72	10.5	4.8	5.94	6.26	7.73	5.68
CaO	5.67	6.79	7.62	2.59	5.88	2.62	10.49	9.49	9.7	11.36	7.81
Na_2O	3.45	3.37	2.64	2.65	4.37	2.76	3.21	2.24	1.91	1.21	2.43
K_2O	2.72	2.11	1.84	0.24	1.07	3.05	0.47	1.37	1.12	0.93	1.22
P_2O_5	0.24	0.18	0.18	0.23	0.2	0.16	0.41	0.75	0.41	0.25	0.54
LOI	0.94	1.4	1.95	4.47	2.15	3.63	1.52	0.88	0.44	0.77	1.19
Sum	99.71	99.75	96.41	101.33	97.27	100.83	99.08	99.29	97.74	98.54	99.5
Mg#	37.30	52.23	50.87	50.71	47.57	59.44	48.09	43.51	45.35	51.06	45.10
CaO/Al_2O_3	0.45	0.56	0.65	0.21	0.48	0.23	0.77	0.80	0.79	0.90	0.57
$Fe_2O_3^t/MgO$	3.55	1.93	2.04	2.05	2.33	1.44	2.28	2.74	2.54	2.02	2.57

(continued)

Table 1 (continued)

Major oxide (wt%)	BG-57	BG-5A	BG-58	BG-58A	BG-60	BG-61	BG-59	BG-79	DG-8(AR)	DG-11	RG-33C
Trace elements (in ppm)											
V	295	329	334	322	298	363	353.95	429.99	396.30	344.10	354.23
Sc	41	43	42	39	30	31	26.25	51.14	42.36	39.26	35.92
Co	38	40	44	45	38	39	31.28	61.32	76.16	69.40	56.60
Cr	67	79	95	42	83	88	71.01	87.83	76.79	69.34	82.37
Rb	40	24	23	22	26	41	11.03	64.98	58.02	24.35	68.23
Ba	515	314	277	35	183	240	79.35	323.31	257.53	91.41	328.19
Sr	107	97	81	nd	81	12	518.81	232.24	349.18	141.85	262.49
Zr	197	133	143	212	141	147	5.94	12.73	8.22	6.79	18.18
Y	27	19	20	14	12	12	39.92	72.09	43.31	28.87	55.71
Nb	12	9	10	22	12	12	40.04	32.66	46.20	20.36	30.90
Ni	nd	nd	nd	nd	nd	nd	14.57	23.37	32.89	36.42	20.73
Cu	nd	nd	nd	nd	nd	nd	38.43	94.56	198.55	108.10	76.17
Zn	nd	nd	nd	nd	nd	nd	73.28	127.78	121.52	87.79	134.13
Ga	nd	nd	nd	nd	nd	nd	23.27	27.63	24.28	20.50	26.51
Cs	nd	nd	nd	nd	nd	nd	0.45	3.95	2.91	0.49	9.77
Hf	nd	nd	nd	nd	nd	nd	0.33	0.87	0.57	0.47	0.41
Ta	nd	nd	nd	nd	nd	nd	9.86	7.26	10.59	7.96	8.71
Pb	nd	nd	nd	nd	nd	nd	8.94	8.03	6.83	7.62	11.20
Th	nd	nd	nd	nd	nd	nd	2.26	3.82	4.16	2.02	6.15

(continued)

Table 1 (continued)

Major oxide (wt%)	BG-57	BG-5A	BG-58	BG-58A	BG-60	BG-61	BG-59	BG-79	DG-8(AR)	DG-11	RG-33C
Rare-earth elements (in ppm)											
La	30	20.1	20	nd	24.3	17.6	21.60	34.46	28.07	15.96	36.56
Ce	66.3	42.4	45.2	nd	47.9	42.4	48.64	78.35	63.58	36.13	76.70
Pr	nd	nd	nd	nd	nd	nd	5.42	8.83	7.08	4.07	8.45
Nd	36	23.8	23.2	nd	23.7	26.5	30.18	50.44	39.32	22.82	45.46
Sm	6.61	4.79	4.66	nd	5.44	5.43	6.35	11.78	8.61	5.02	9.92
Eu	1.5	1.24	1.24	nd	1.4	1.61	2.27	3.72	2.80	1.75	2.83
Gd	6.1	4.53	4.69	nd	4.61	4.87	7.69	15.04	10.23	6.17	12.36
Tb	nd	nd	nd	nd	nd	nd	1.20	2.35	1.55	0.96	1.86
Dy	6.05	4.67	4.83	nd	4.49	4.32	6.15	11.85	7.45	4.77	9.16
Ho	nd	nd	nd	nd	nd	nd	1.31	2.46	1.50	0.99	1.85
Er	2.87	2.82	2.75	nd	2.5	2.68	4.15	7.55	4.59	3.08	5.66
Tm	nd	nd	nd	nd	nd	nd	0.65	1.22	0.73	0.50	0.87
Yb	3.84	3.13	3.36	nd	2.38	2.6	3.19	6.35	3.75	2.68	4.44
Lu	0.25	0.24	0.25	nd	0.14	0.17	0.43	0.93	0.57	0.42	0.60

nd represents not determined

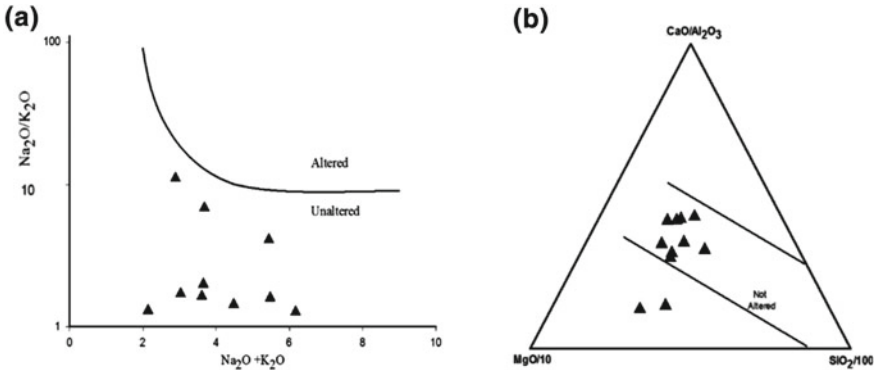

Fig. 4 **a** Na_2O/K_2O versus Na_2O+K_2O binary diagram (after Miyashiro 1975), **b** CaO/Al_2O_3–MgO/10-SiO_2/100 ternary plot (Schweitzer and Kroner 1985) for the Bomdilametabasic rocks of Lesser Himalaya

For this reason, the elements which are known to be immobile or less mobile during secondary alteration processes such as rare earth elements (REE), HFSE as well as Ti, P, Cr, Ni can be used for petrogenetic interpretation (Winchester and Floyd 1977; Saunders et al. 1980; Rollinson 1993).

4.3 Geochemical Characteristics

The studied metabasic rocks have restricted range of SiO_2 (45–53wt%). The concentration of other major elements such as; CaO, Al_2O_3, TiO_2, P_2O_5 and MnO ranges from (7.18–11.36 wt%), (11.2–13.01), (2.5–4.0 wt%), (0.16–0.8 wt%) and (0.15–0.25 wt%) respectively. In total alkali silica (TAS) classification diagram after (Le Maitre 2002) the studied Bomdila and Rupa metabasic rocks plot mainly in the field of basalt to basaltic-andesite (Fig. 5). Most of the samples have Nb/Y ratios <0.7 indicating their sub alkaline affinity (Pearce and Gale 1977).

In YTC (Y = Y + Zr, Ti = TiO_2 wt% × 100, C = Cr) ternary diagram (Davies et al. (1979), most of the studied samples plot along and above the tholeiitic trend (Fig. 6a). This tholeiitic nature is very clearly observed on Jensen's cation triangular plot (Al–(Fe + Ti)–Mg) (Jensen 1976), in which studied samples plot in Fe-tholeiitic field (Fig. 6b).

Various binary variation diagrams have been plotted to understand the crystallization behavior of studied rock samples (Fig. 7). In these binary plots, we use some known mobile elements e.g., CaO, Na_2O, K_2O and Sr and less mobile or immobile elements e.g., SiO_2, Al_2O_3, TiO_2, P_2O_5, Y, Yb, La, Ce and Nb (Pearce and Cann 1973; Flyod and Winchester 1978; Rollinson 1993) against MgO. These plots show overall magmatic trends, suggesting that these elements are immobile. The studied samples show systematic increase in SiO_2, Al_2O_3, CaO, Na_2O and P_2O_5 with

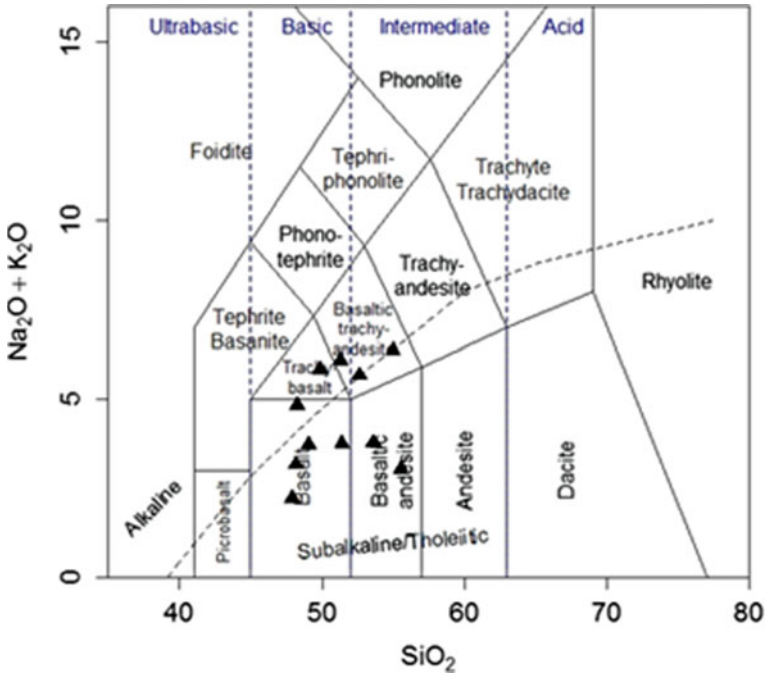

Fig. 5 Total Alkali Silica (TAS) classification diagram (after Le Maitre 2002) for the classification of the metabasic rocks of the Lesser Himalaya from Bomdila area

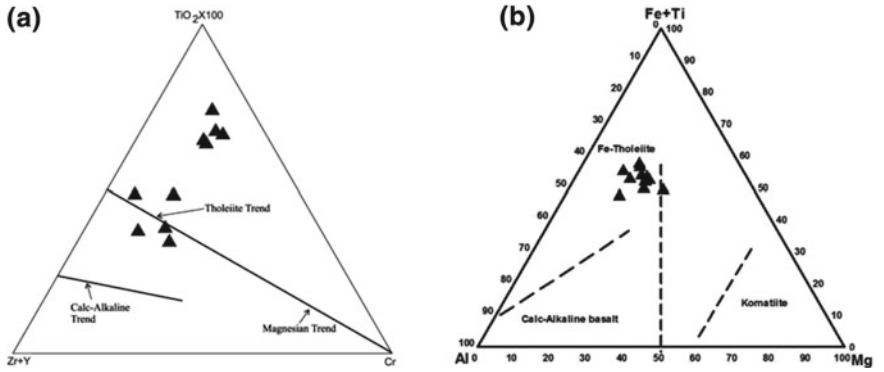

Fig. 6 **a** Y (Zr + Y)−T ($TiO_2 \times 100$)−C (Cr) ternary plot (after Davies et al. 1979) showing the tholeiitic affinity of the basic rocks and **b** Ternary cation% Al–(Fe + Ti)–Mg plot (after Jensen 1976) for Bomdilametabasic rocks

decreasing MgO, whereas TiO_2 show increasing trend with MgO increase. These trends suggest fractionation of mafic magma wherein minerals like olivine, pyroxene and feldspar have fractionated earlier followed by Fe–Ti oxides. Also, in Fig. 7,

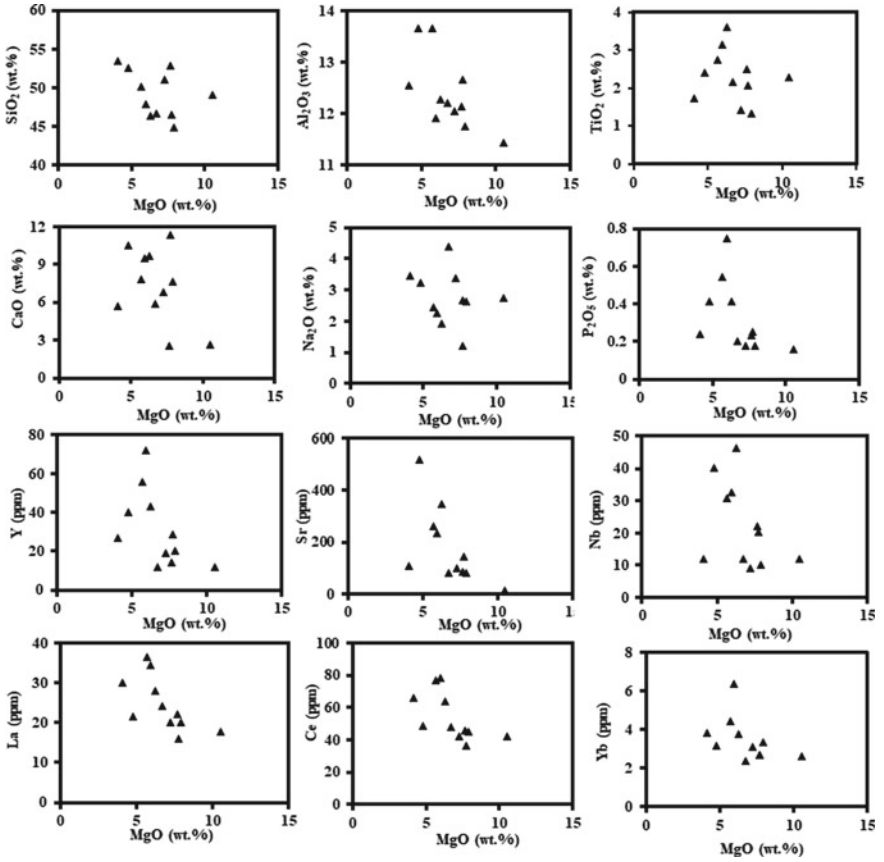

Fig. 7 Harker variation diagrams for Bomdilametabasic rocks showing major and trace element variation against MgO

trace elements such as Y, La, Ce, Nb, Yb and Sr show negative correlation with MgO which is consistent with crystallization of minor minerals at later stage (Srivastava 2012). Negative correlation of Sr with MgO is consistent with high level plagioclase fractionation. The higher concentration of $Fe_2O_3^t$ (10–16 wt%) and TiO_2 (1.32–3.6 wt%) in the studied samples indicates fractional crystallization of Mg and Ca—rich minerals at depth, facilitating late stage crystallization of Fe–Ti oxides at higher levels (Ahmad and Tarney 1991).

The chondrite normalized REE and primitive mantle-normalized incompatible multi-element patterns for the present metabasic rocks are shown in Fig. 8. The studied samples have sub-parallel REE patterns with enriched LREE [$(La/Yb)_N$ ratio 3.89–7.3] and slightly depleted HREE patterns with low Eu negative anomaly (Eu/Eu* = 0.72–0.96) (Fig. 8a), reflecting their generation from similar mantle sources. Also the enrichment of large ion lithophile elements (LILE) is evident in

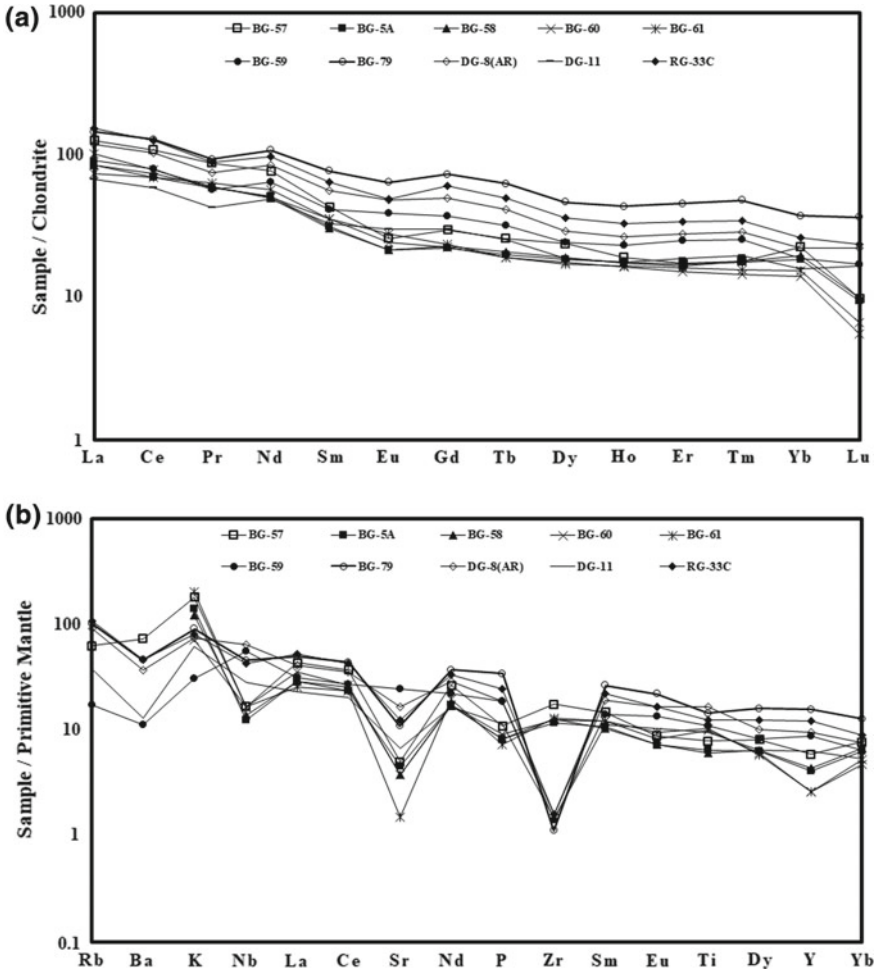

Fig. 8 **a** Chondrite-normalized REE patterns and **b** primitive mantle normalized multi- element patterns for Bomdilametabasic samples. Chondrite and primitive mantle normalized values are after Sun and McDonough (1989)

multi-element patterns (Fig. 8b) with distinct negative Sr anomaly in all the samples but selective depletion of HFSE. Some samples are depleted in Nb, P and Y whereas few samples depict Zr negative anomaly. This variable depletion of HFSE in the studied rocks is likely due to differences in depth and degrees of partial melting (Ahmad et al. 1999). Observed prominent negative Sr anomaly in studied samples indicates shallow level fractionation of plagioclase feldspar during evolution of the melt (Tarney and Jones 1994) which is also corroborated by the low Eu negative anomaly in few samples.

The enriched LREE-LILE and depleted HFSE patterns in the studied metabasic rock (Fig. 8b) may be attributed to either enriched mantle source or crustal contamination (Ahmad and Tarney 1991). Various geochemical criteria are often used to monitor the possibility of crustal contamination (Rollinson 1993). The incompatible element ratios such as Nb/La and Nb/Ce are proxy indicators used to constrain the influence of crustal inputs on the mafic rock compositions (Li et al. 2006; Sandeman et al. 2006). The Nb/La values of 0.40–1.85 (average 0.83) and Nb/Ce values of 0.18–0.82 (average 0.37) of studied metabasic samples are higher than average bulk crustal composition of 0.69 and 0.33 respectively of Taylor and McLennan (1985) reflecting crustal contamination. However, their Fe-enrichment, lower Th/Ta ratio (<0.71) and higher Ti/Zr ratios (>52) does not support the above interpretation (Arndt and Jenner 1986). Furthermore, their regular REE patterns are against crustal contamination which would otherwise exhibit steeper slope for LREE compared to HREE. Therefore, the observed trace element characteristics of the studied metabasic rocks are primarily inherited from a LREE-LILE enriched mantle source depleted in HFSE (Ahmad and Tarney 1991).

5 Discussion

5.1 Petrogenesis

Due to the immobile and incompatible behavior of trace elements during post-crystallization alteration processes, the incompatible trace element ratios and multi-element spidergrams are commonly useful in magma identification and source characterization of any magma suite (Pearce 1982, 2008; Rollinson 1993). Ratios of highly incompatible trace elements such as Nb/La, Ce/Nd, Zr/Nb, Ta/Th etc. do not change significantly due to moderate degrees of melting and fractional crystallization so are expected to reflect the source characteristics (Saunders et al. 1988; Ahmad and Tarney 1991; Petterson and Windley 1992; Condie 1997; Srivastava et al. 2008; French and Heaman 2010). Some of the important characters like low magnesium numbers (mostly < 60) and negative Sr as well as Eu anomalies of the studied metabasic rocks suggest that fractional crystallization has played a role in the generation of these rocks. The positive correlation of CaO/Al_2O_3 versus $Fe_2O_3^t/MgO$ (Table 1) further indicates that olivine, pyroxene and plagioclase were the main fractionating phases. However, a large variation in incompatible element ratios (e.g., La/Yb, Zr/Y, Ti/Y, Zr/Nb) in the studied rocks cannot be explained by crystal fractionation alone. In Zr/Y versus Zr plot (Fig. 9), large variation in Zr/Y ratio is depicted with increasing Zr abundance. Generally, pyroxene and amphibole fractionation is believed to slightly increase this ratio in basaltic rocks (Floyd 1993) however, this ratio is more sensitive to variable degrees of partial melting of similar mantle sources (Ahmad et al. 1999). Therefore, such large variation of Zr/Y and other incompatible element ratios in studied rocks depicts different degrees of partial melting of a similar mantle

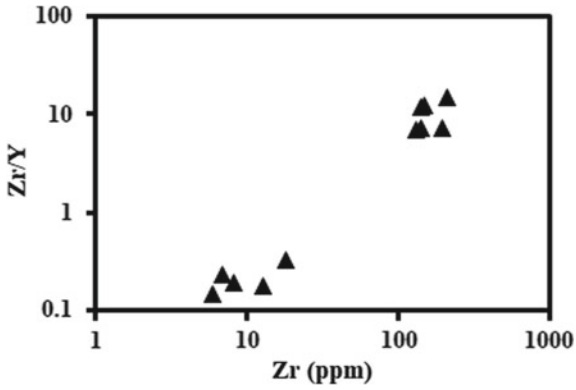

Fig. 9 Binary plot of Zr/Y versus Zr (after Sun and Nesbitt 1977) for the Bomdilametabasics from Lesser Himalaya

source. Similar observations were observed in Garhwal dykes of Lesser Himalaya by Ahmad et al. (1999). It may be concluded from the above discussion that the studied metabasic rocks were derived due to different degrees of partial melting of an enriched mantle source subsequently followed by fractionation.

The studied samples plotted on $(La/Yb)_N$ versus $(La)_N$ plot (Fig. 10) that further supports the inference that these rocks were generated by different degrees of partial melting of a common mantle source. In general, on this type of plot, a linear relationship will be defined by the samples if they are derived by different degrees of partial melting of a common source however, the samples may shift horizontally to higher X-axis values because of crystal fractionation (Feigenson et al. 1983; Bradshaw et al. 1993; Vimal et al. 2012; Hirahara et al. 2015). A broad positive linear pattern is exhibited by the studied rocks in $(La/Yb)_N$ versus $(La)_N$ diagram, indicating that they were formed by different degrees of melting of a source with similar $(La/Yb)_N$. Lower degrees of melting resulted the samples with higher La and La/Yb whereas samples with lower La and La/Yb have formed by higher degree of melting.

To know the depth of mantle melting incompatible element ratio Sm/Yb can trace the presence or absence of residual garnet because fractional crystallization has no effect on it (McKenzie and O'Nions 1991; Zi et al. 2008). Yb is compatible in garnet as compared to Sm and La which are incompatible so are enriched in melts during low degrees of partial melting. The high La/Sm and Sm/Yb ratios greater than 1 in studied samples indicate a magma origin involving low degrees of melting of a garnet bearing mantle source.

The studied metabasic rocks of Lesser Himalayan Sequence are compared for their geochemical characters with two other occurrences from the western Arunachal Himalaya (Fig. 11). Strikingly similar REE patterns were observed for studied metabasics and metabasic of Bikramaditya Singh and Singh (2013) from Lesser Himalaya, however, both are quite distinct with Sela group metabasics of Higher Himalayan Crystallines. This observation suggests that the metabasic rocks reported from the Lesser Himalaya and Higher Himalaya have different petrogenetic history. Srivastava et al. (2009) suggested that the Sela group metabasics of Higher

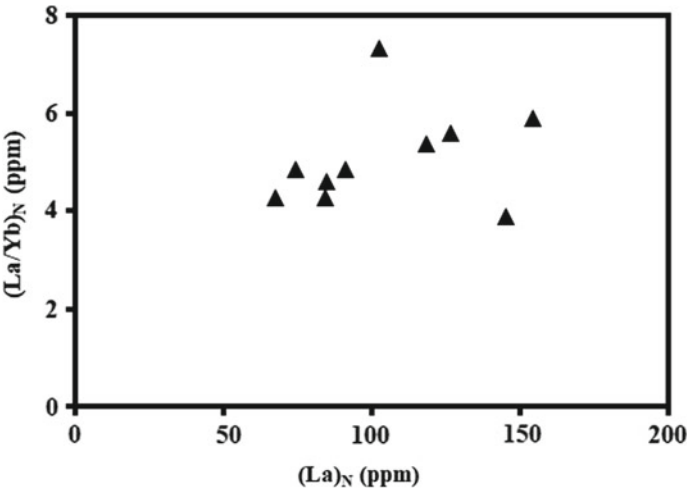

Fig. 10 $(La/Yb)_N$ versus $(La)_N$ for Bomdilametabasic rocks from Lesser Himalaya showing the positive relationship (normalized to primitive mantle after Sun and McDonough 1989)

Himalaya are derived from a depleted asthenospheric mantle and are related to Western Himalayan metabasic rocks such as Vaikrita amphibolites (Ahmad et al. 1999). Srivastava and Sahai (2001) suggested the same for the mafic magmatic rocks reported from the Central Crystallines of the Bhagirath–Yamuna valleys. Recently, Srivastava and Samal (2018) reported high Ti mafic intrusives from the western Arunachal Himalaya with inclined REE patterns similar to the present studied metabasic rocks indicating enriched mantle sources.

The studied metabasic rocks have striking similarity with other Proterozoic metabasic rocks of Lesser Himalaya like Chail and Jutogh amphibolites, Garhwal volcanics and dykes of Ahmad (2008) and metabasics of Bikramaditya Singh and Singh (2013) in terms of normalized REE patterns (Fig. 12), multi-element patterns and some important incompatible element ratios. Also they show similar geochemical characteristics to that of high Ti mafic intrusives of Srivastava and Samal (2018). All these rocks show tholeiitic nature, overall low Mg-numbers (reflecting their evolved nature), enriched LREE-LILE and depleted HFSE characteristics. These geochemical signatures are similar with most of the continental rift volcanics and Proterozoic dyke swarms (Thompson et al. 1983; Weaver and Tarney 1984; Tarney 1992; Hawkesworth et al. 1993).

5.2 Tectonic Setting

An attempt was made to elucidate the tectonic setting of emplacement of Bomdila metabasic rocks. It has been suggested that the basalts from different tectonic set-

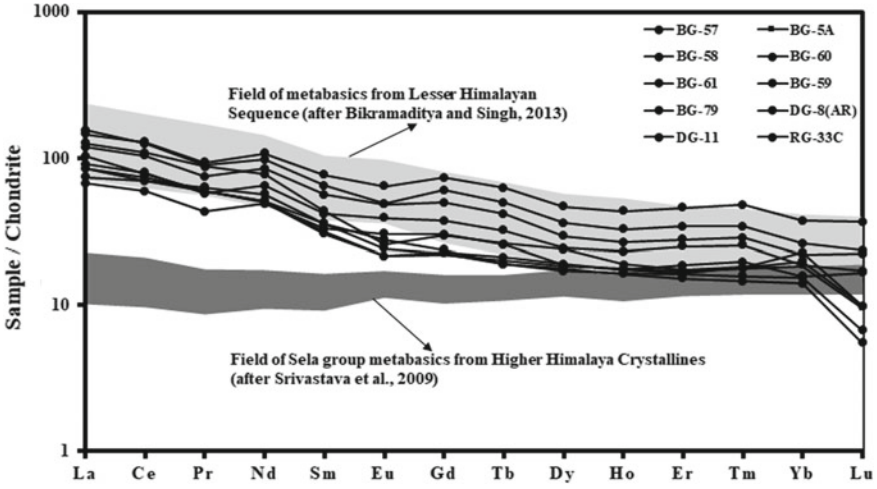

Fig. 11 Comparison of rare-earth element patterns of metabasic rocks (present study) from Lesser Himalayan sequences with Sela group metabasic rocks of Higher Himalayan Crystallines (Srivastava et al. 2009) and metabasic rocks of Lesser Himalayan sequences (after Bikramaditya Singh and Singh 2013)

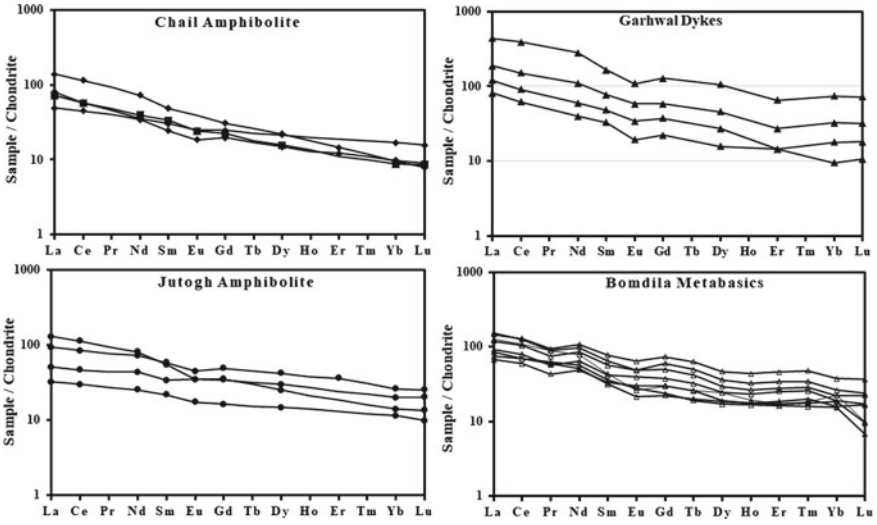

Fig. 12 Comparison of rare-earth element patterns of Bomdilametabasic rocks (present study) with Chail amphibolites, Garhwal dykes and Jutoghamphibolites of Lesser Himalaya (dataafter Ahmad 2008)

tings may often be distinguished by the relative abundances of 'immobile' elements such as Ti, P, Zr, Nb, Y, Cr and REE (Pearce and Cann 1973; Pearce 1975). Saunders et al. (1980) have observed that the basalts from active and remnant arcs are

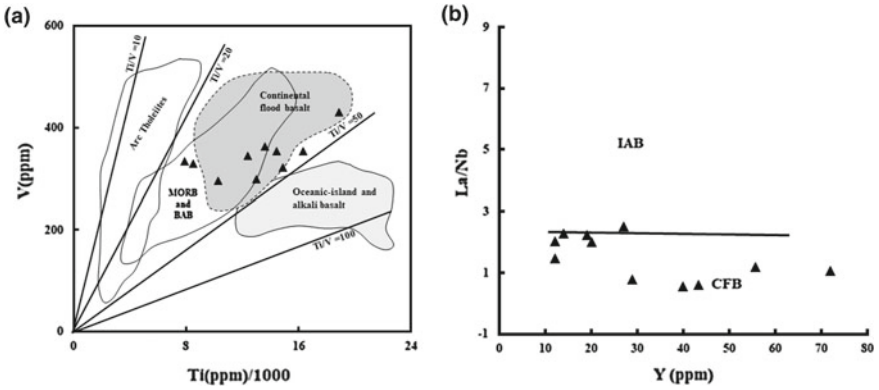

Fig. 13 **a** Ti/1000 versus V diagram (after Shervais 1982) and **b** La/Nb versus Y diagram (after Floyd et al. 1991) distinguishing Bomdilametabasics as continental flood basalts. CFB = continental flood basalts; IAB = island arc basalts

characterized by higher abundance of LILE (Cs, Rb, K, Ba, Sr, Th, U) relative to HFSE (Ti, P, Zr, Hf, Nb and Ta) than ocean ridge basalts. Wang and Glover III (1992) suggested that particularly the continental rift basalts invariably plot outside the within-plate field. The present studied samples are characterized by high V concentration (295–429 ppm), Ti/V > 20, lower La/Nb (0.54–2.50), Zr (<250 ppm) and Ti/Y < 410 all reflect continental Parana flood basalt geochemical characteristics (Erlank et al. 1988). Incompatible immobile element concentrations in basalts are proxy indicators for determining their tectonic environment of eruption especially ratios of La/Nb, Ti/V and Y, V concentrations (Winchester and Floyd 1976; Shervais 1982; Floyd et al. 1991; Kuzmichev et al. 2005). In Ti/1000 versus V tectonic discrimination diagram of Shervais, (1982), the Ti and V are relatively immobile up to high grade granulite facies of metamorphism (Rollinson 1993). In studied metabasic rocks, the Ti/V ratio ranges from 24 to 46 and plots within continental flood basalt field (Fig. 13a). In La/Nb versus Y plot of Floyd et al. (1991) the Bomdila metabasics also plot in the field of continental flood basalts (Fig. 13b). As discussed earlier the enrichment of LREE-LILE and depletion in HFSE also indicates rift tectonic environment. Also the low Nb/La ratio (<1) of studied samples is a characteristic feature of many continental flood basalts like Parana, Karoo and Deccan.

The continental rift tectonic scenario for studied metabasic rocks is corroborated by their remarkable similarities in trace element characteristics with Lesser Himalayan Mandi-Darla-Rampur volcanics of Himachal Pradesh (Ahmad and Bhat 1987; Bhat and Le Fort 1992), Garhwal volcanics (flows and dykes), Chail and Jutogh amphibolites of Utrakhand (Ahmad and Tarney 1991, Ahmad et al. 1999), Proterozoic Basal Aravalli volcanics of NW Indian shield (Ahmad and Rajamani 1991; Ahmad and Tarney 1994) and also with high Ti mafic intrusives (HTMI) from western Arunachal Himalaya (Srivastava and Samal 2018).

6 Conclusions

The Bomdila metabasics occur as sills and dykes in the Rupa and Bomdila group of rocks in Lesser Himalayan Sequence of the western Arunachal Himalaya, and show amphibolite grade metamorphism. These rocks are chemically classified as sub-alkaline tholeiites and contain hornblende and plagioclase feldspar in major proportion. The studied rocks have similar $(La/Yb)_N$ ratios (4.27–5.91) but varying $(La)_N$ (67–154) values indicating that they were formed by different degrees of melting of a source with similar $(La/Yb)_N$ ratios. Presence of enriched LREE and LILE and depleted HFSE concentrations suggest that these rocks were generated from enriched mantle source comparable to sub-lithospheric mantle in rift tectonic environment. The studied metabasic rocks have striking similarity with other Proterozoic metabasic rocks of the Lesser Himalaya like Chail and Jutogh amphibolites, Garhwal volcanics and dykes in terms of normalized REE patterns, multi-element patterns and some important incompatible element ratios, thus pointing towards a strong magmatic event in rift tectonic environment during the Proterozoic time along the Lesser Himalayas, as also suggested by Srivastava and Samal (2018).

Acknowledgements We are thankful to the Chairpersons, Department of Geology, AMU, Aligarh and Department of Earth Sciences, University of Kashmir, Srinagar for providing necessary facilities to carry out this work. Dr. N. K. Saini and Dr. A. K. Singh, WIHG, Dehradun and Dr. V. Balaram, NGRI, Hyderabad are thankfully acknowledged for analytical facility. SAR is thankful to the DST, New Delhi for financial support in the form of a major project. The authors are also thankful to anonymous reviewers for their constructive comments that helped us to improve the quality of the manuscript. We are thankful to Profs. R. K. Srivastava, Richard and Peng for editorial handling.

References

Acharyya SK (1971) Structure and stratigraphy of the Darjeeling frontal zone, Eastern Himalaya. Misc Publ Geol Survey of India 24:71–90

Acharyya SK, Ghosh SC, Ghosh RN, Shah SC (1975) The continental Gondwana Group and associated marine sequences of Arunachal Pradesh (NEFA), Eastern Himalaya. Himalayan Geol 5:60–82

Ahmad T, Bhat MI (1987) Geochemistry and petrogenesis of the Mandi-Darla volcanics, north western Himalayas. Precambr Res 37:231–256

Ahmad T, Tarney J (1991) Geochemistry and petrogenesis of Garhwal volcanics: implications for evolution of the north Indian lithosphere. Precambr Res 50:69–88

Ahmad T, Rajamani V (1991) Geochemistry and petrogenesis of the basal Aravalli volcanics near Nathdwara, Rajasthan. Precambr Res 49:327–340

Ahmad T, Tarney J (1994) Geochemistry and petrogenesis of late Archean Aravalli volcanics, basement enclaves and granitoids, Rajasthan. Precambr Res 65:1–23

Ahmad T, Mukherjee PK, Trivedi JR (1999) Geochemistry of Precambrian mafic magmatic rocks of the Western Himalaya, India: petrogenetic and tectonic implications. Chem Geol 160:103–119

Ahmad T (2008) Precambrian mafic magmatism in the Himalayan mountain range. J Geol Soc India 72:85–92

Arndt NT, Jenner GA (1986) Crustally contaminated komatiites and basalts from Kambalda, Western Australia. Chem Geol 56:229–255

Balaram V, Ramesh SL, Anjaiah KV (1996) New trace element and REE data in thirteen GSF reference samples by ICP-MS. Geostand Geoanal Res 20:71–78
Bhalla JK, Bishui PK (1989) Geochronology and geochemistry of granite emplacement and metamorphism in northeastern Himalaya. Rec Geol Surv India 122:18–20
Bhat MI (1984) Abor volcanics: further evidence for the birth of the Tethys Ocean in the Himalyan segment. J Geological Society of London 141:763–775
Bhat MI, Ahmad T (1990) Petrogenesis and the mantle source characteristics of the Abor volcanic rocks, eastern Himalayas. Geological Society of India 36:227–246
Bhat MI, Le Fort P (1992) Sm-Nd age and Petrogenesis of Rampur meta-volcanic rocks, NW-Himalayas: Late Archaean relicts in the Himalayan belt. Precambr Res 56:191–210
Bikramaditya Singh RK, Singh AK (2013) Geochemistry and petrogenesis of metabasic rocks from the Lesser Himalayan Crystallines, western Arunachal Himalaya, northeast India. Geosci J 17:27–41
Bradshaw TK, Hawkesworth CJ, Gallagher K (1993) Basaltic volcanism in the Southern Basin and Range: no role for a mantle plume. Earth and Planetary Science Letters 116:45–62
Bhushan SK, Bindal CM, Aggarwal RK (1991) Geology of Bomdila group in Arunachal Pradesh. Himalayan Geol 2:207–214
Cann JR (1970) Rb, Sr, Y, Zr and Nb in some ocean floor basaltic rocks. Earth Planet Sci Lett 10:7–11
Condie KC, Viljoen MJ, Kable EJD (1977) Effects of alteration on element distributions in Archean tholeiites from the Barberton greenstone belt, South Africa. Contrib Miner Petrol 64:75–89
Condie KC, Sinha AK (1996) Rare earth and other trace element mobility during mylonitization: a comparison of the Brevard and Hope Valley shear zones in the Appalachian Mountains, USA. J Met Geol 14:213–226
Condie KC (1997) Sources of Proterozoic mafic dyke swarms: constraints from Th/Ta and La/Yb ratios. Precambr Res 81:3–14
Davies JF, Grant RWE, Whitehead RES (1979) Immobile trace elements and Archean volcanic stratigraphy in the Timmins mining area, Ontario. Can J Earth Sci 16:305–311
Dikshitulu GR, Pandey BK, Krishna V, Raju RD (1995) Rb-Sr systematics of granitoids of the central gneissic complex, Arunachal Himalaya: implications on tectonism, stratigraphy and source. Geological Society of India 45:51–56
Erlank AJ, Duncan AR, Marsh JS (1988) A laterally extensive geochemical discontinuity in subcontinental Gondwana lithosphere. In: Proceedings of the V Conference on Geochemical Evolution of the Continental Crust, Brazil, pp 1–10
Feigenson MD, Hofmann AW, Spera FJ (1983) Case studies on the origin of basalt. Contrib Miner Petrol 84:390–405
Floyd PA, Winchester JA (1978) Identification and discrimination of altered and metamorphosed volcanic rocks using immobile elements. Chem Geol 21:291–306
Floyd PA, Kelling SL, Gokcen SL, Gokcen N (1991) Geochemistry and tectonic environment of basaltic rocks from the Misis ophiolitic melange, south Turkey. Chem Geol 89:263–280
Floyd PA (1993) Geochemical discrimination and petrogenesis of alkalic basalt sequences in part of the Ankara mélange, central Turkey. Geol Soc London 150:541–550
French JE, Heaman LM (2010) Precise U–Pb dating of Paleoproterozoic mafic dyke swarms of the Dharwar craton, India: implications for the existence of the Neoarchean supercraton Sclavia. Precambr Res 183:416–441
Hirahara Y, Kimura J-I, Senda R, Miyazaki T, Kawabata H, Takahashi T, Chang Q, Vaglarov BS, Sato T, Kodaira S (2015) Geochemical variations in Japan Sea back-arc basin basalts formed by high-temperature adiabatic melting of mantle metasomatized by sediment subduction components. Geochem Geophy Geosys 16:1324–1347
Hawkesworth CJ, Gallagher K, Pearson G, Turner SP, Calsteren V (1993) The continental lithosphere: a geochemical perspective. An Acad Bras Ci 65:199–225
Jain AK, Thakur VC (1978) Abor volcanics of the Arunachal Himalaya. Geol Soc India 19:335–349

Jensen LS (1976) A new cation plot for classifying subalkalic volcanic rocks. Min Nat Res Ontario Div Min Misc paper 66:20
Kumar G (1997) Geology of Arunachal Pradesh. Geological Society of India, Bangalore, p 217
Kuzmichev A, Kroner A, Hegner E, Dunyi L, Yusheng W (2005) The Sheshkhid ophiolite, northern Mongolia: a key to the reconstruction of a Neoproterozoic island-arc system in central Asia. Precambr Res 138:125–150
Lafleche MR, Dupuy C, Bougault H (1992) Geochemistry and petrogenesis of Archean volcanic rocks of the southern Abitibi Belt, Quebec. Precambr Res 57:207–241
Le Maitre RW (2002) Igneous rocks: a classification and glossary of terms, 2nd edn. Cambridge University Press, Cambridge, p 236
Li XH, Li ZX, Wingate MTD, Chung SL, Liu Y, Lin GC, Li WX (2006) Geochemistry of the 755 Ma Mundine well dyke swarm, North Western Australia: part of a Neoproterozoic mantle superplume beneath Rodinia. Precambr Res 146:1–15
McKenzie D, O'Nions RK (1991) Partial melt distributions from inversion of rare earth element concentrations. J Petrol 32:1021–1091
Miyashiro A (1975) Classification, characteristics, and origin of ophiolites. J Geol 83:249–281
Pearce JA, Cann JR (1973) Tectonic setting of basic volcanic rocks determined using trace element analyses. Earth Planet Sci Lett 19:290–300
Pearce JA (1975) Basalt geochemistry used to investigate past tectonic environments on Cyprus. Tectonophysics 25:41–67
Pearce JA, Gale DH (1977) Identification of ore deposition environment from trace element geochemistry. Geol Soc Lond Spec Publ 7:14–24
Pearce JA (1982) Trace element characteristics of lavas from destructive plate boundaries. In: Thorpe RS (ed) Orogenic Andesites. Wiley, Chichester, UK, pp 528–548
Pearce JA (2008) Geochemical fingerprinting of oceanic basalts with applications to ophiolite classification and the search for Archean oceanic crust. Lithos 100:14–48
Petterson MG, Windley BF (1992) Field relations, geochemistry and petrogenesis of the Cretaceous basaltic Jutal dykes, Kohistan, northern Pakistan. J Geol Soc Lond 149:107–114
Rashid SA, Islam N (2016) Geochemical characteristics of proterozoic mafic dykes from the Bomdila Group of rocks, NE Lesser Himalaya, India. Acta Geologica Sinica 90:122
Rollinson HR (1993) Using geochemical data: evaluation, presentation, interpretation. Longman Scientific Technical, Essex, UK, p p344
Roychowdhury J (1984) The Abor group of rocks in Arunachal Pradesh. Record Geol Surv India 113:48–57
Sahai A, Srivastava RK (1997) Structural and geochemical characteristics of amphibolites from the Bhagirathi and Yamuna valleys of Main Central Thrust Zone, Garhwal Himalaya. J Himalayan Geol 18:191–201
Sandeman HA, Hanmer S, Tella S, Arimetage AA, Davis WJ, Ryan JJ (2006) Petrogenesis of Neoarchaean rocks of the Mc Quoid supracrustal belt: a back-arc setting for the northwestern Hearne Subdomain, western Churchill Province, Canada. Precambr Res 144:140–165
Saunders AD, Tarney J, Weaver SD (1980) Transverse geochemical variations across the Antarctic Peninsula: implications for the genesis of calc-alkaline magmas. Earth Planet Sci Lett 46:344–360
Saunders AD, Norry MJ, Tarney J (1988) Origin of MORB and chemically depleted mantle reservoirs: trace element constraints. In: Menzies MA, Cox KG (eds) Oceanic and continental lithosphere: similarities and differences. J Petrol, pp 415–455
Schweitzer J, Kroner A (1985) Geochemistry and petrogenesis of early Proterozoic intra-cratonic volcanic rocks of the Ventersdorp Supergroup, South Africa. Chem Geol 51:265–288
Sengupta S, Acharyya SK, De Smeth JB (1996) Geochemical characteristics of the Abor volcanics, NE Himalaya, India: nature and early Eocene magmatism. J Geol Soc London 153:695–704
Shervais JW (1982) Ti–V plots and petrogenesis of modern and ophiolitic lavas. Earth Planet Sci Lett 59:108–118
Singh AK (2006) Petrography, geochemistry and petrogenesis of Abor Volcanics, Eastern Himalayan Syntaxial Bend. Himalayan Geol 27:163–181

Singh AK, Bikramaditya Singh RK (2012) Petrogenetic evolution of the felsic and mafic volcanic suite in the Siang window of Eastern Himalaya, Northeast India. Geoscience Frontier 3:613–634
Singh S (1993) Geology and tectonics of the eastern syntaxial bend, Arunachal Himalaya. J Himalayan Geol 4:149–163
Srinivasan A (2001) Stratigraphy and structure of low grade meta-sedimentaries in eastern Bhutan and western Arunachal Pradesh. J Himalayan Geol 22:83–98
Srivastava RK, Sahai A (2001) High-Field Strength element geochemistry of mafic intrusive rocks from the Bhagirathi and Yamuna valleys, Garhwal Himalaya, India. Gondwana Res 4:455–463
Srivastava RK (2012) Petrological and geochemical studies of paleoproterozoic mafic dykes from the Chitrangi Region, Mahakoshal Supracrustal Belt, Central Indian Tectonic Zone: Petrogenetic and tectonic significance. J Geol Soc India 80:369–381
Srivastava RK, Samal AK (2018) Geochemical characterization, petrogenesis and emplacement tectonics of Paleoproterozoic high-Ti and low-Ti mafic intrusive rocks from the western Arunachal Himalaya, Northeastern India and their possible relation to the ~1.9 Ga LIP event of the Indian shield. Geological Journal in press. https://doi.org/10.1002/gj.3172
Srivastava RK, Sivaji C, Chalapathi Rao NV (2008) Indian Dyke: geochemistry geophysics and geochronology. Narosa Publishing House Ltd., New Delhi, p p626
Srivastava RK, Srivastava HB, Srivastava V (2009) Petrology and geochemistry of Proterozoic olivine tholeiite intrusives from the Central Crystallines of the western Arunachal Himalaya, India: evidence for a depleted mantle. Curr Sci 97:1355–1361
Sun SS, Nesbitt RW (1977) Chemical heterogeneity of the Archean mantle composition of the bulk earth and mantle evolution. Earth Planet Sci Lett 35:429–448
Sun SS, McDonough WF (1989) Chemical and isotopic systematics of oceanic basalts: implications for mantle composition and processes. Magmatism in the ocean basins 42:313–345
Tarney J (1992) Geochemistry and significance of mafic dyke swarms in the Proterozoic. In: Condie KC (ed) Proterozoic crustal evolution. Elsevier, Amsterdam, pp 151–179
Tarney J, Jones CE (1994) Trace element geochemistry of orogenic igneous rocks and crustal growth models. J Geol Soc London 151:855–868
Taylor SR, McLennan SM (1985) The continental crust: its composition and evolution. Blackwell Publishers, Oxford, p p312
Thakur VC (1986) Tectonic zonation and tectonic framework of Eastern Himalaya. Science de la Terre Memoir 47:347–360
Thompson RN, Morrison MA, Dickin AP, Henery GL (1983) Continental flood basalts—Arachnids rule OK. In: Hawkesworth CJ, Norry MJ (eds) Continental Basalts and Mantle Xenoliths. Shiva Publication Limited, Cheshire, pp 58–85
Verma PK, Tandon SK (1976) Geological observations in a part of the Kameng district, Arunachal Pradesh (NEFA). J Himalayan Geol 6:259–286
Vimal R, Banerjee R, Gupta S, Krishna V, Achar KK, Babu PR, Parihar PS, Maithani PB (2012) Geochemistry and Sr and Pb isotope systematics of basement granitoids from north and west of Palnad Sub-basin, Guntur and Nalgonda districts, Andhra Pradesh. J Appl Geochem 14:295–315
Wang P, Glover L (1992) A tectonics test of the most commonly used geochemical discriminant diagrams and patterns. Earth-Sci Rev 33:111–131
Weaver BL, Tarney J (1984) Empirical approach to estimating the composition of the continental crust. Nature 310:575–577
Winchester JA, Floyd PA (1977) Geochemical discrimination of different magma series and their differentiation products using immobile elements. Chem Geol 20:325–344
Zi J, Fan W, Wang Y, Peng T, Guo F (2008) Geochemistry and petrogenesis of the Permian mafic dykes in the Panxi region, SW China. Gondwana Research 14(3):368–382